Fusion of Difference Images for Change Detection

Deepthy.R
PG Scholar, Department of ECE
Kumaraguru College of Technology
Coimbatore-641049. Tamilnadu
ardeepthy3688@gmail.com

A.Vasuki, Ph.D
Professor, Department of ECE
Kumaraguru College of Technology
Coimbatore-641049. Tamilnadu
Vasuki.a.ece@kct.ac.in

ABSTRACT

The Land use/ Land cover change in urban areas and the difference of the earth surface after the flood can be detected from remote sensing images by performing image differencing algorithms. Although many algorithms were proposed to generate difference images, the results are inconsistent. In order to integrate the merits of difference algorithms, fusion techniques are used to merge multiple difference images. The image fusion algorithms applied here are based on Principal Component Analysis and Discrete Wavelet Transform. Principal Component Analysis is the unsupervised technique, the change is guaranteed to be preserved in the major component images. In Wavelet based method, image fusion is performed at the pixel level and the details from source images can be reserved at various scales. The algorithms are implemented on the satellite images and results are presented.

GENERAL TERMS

Image Differencing, Change detection, Image fusion, Principal Component Analysis, Discrete Wavelet Transform.

1. INTRODUCTION

The changes are detected by comparing multiple remote sensing images of the same ground area acquired at different times usually. However, conventional change detection methods such as differencing and ratioing [4] do not explicit spectral characteristics of the different land cover changes since they employ only one spectral channel. Besides, complete information about the change is needed, including positions and spatial extent as well as the precise nature of change. Therefore, recently, attention has been focused on machine learning techniques such as Post Classification Comparison (PCC)[5], Artificial Neural Networks (ANN)[16] since they use all spectral channels and provide complete information about land cover changes. A straightforward approach, called Support Vector Machines (SVM)[16] is used. In case that the prior knowledge is unavailable these ANN and SVM are not applicable. The analysis and processing directly or indirectly on the original multi-temporal images to obtain change information, such as image differencing, Principal Component Analysis (PCA)[19], Change Vector Analysis (CVA)[18], Spectral Ratioing and so on are used. Flood area detection using multi-modal remote sensing, which is a good example of change detection to real disaster monitoring.

However, no existing approach is optimal and applicable to all cases, so it is always a big challenge to select a suitable algorithm for a specific application [5],[12]. Therefore, it is an important to build an appropriate unsupervised change detection model to process multi-temporal remotely sensed images and implement an efficient monitoring scheme for urban expansion, land cover change, flood detection and disaster monitoring where no or little prior knowledge is available. By combining different Spectral Change Difference (SCD) images and the corresponding change detection results, the proposed approach can take full take advantage of their merits to improve the ability to identify and extract changes, and reduce the uncertainty remaining after using a single difference image.

In section II, we present five different algorithms for generating difference images.. In section III, we present the Principal Component Analysis algorithm(PCA) for image fusion.. In section IV, we present the Discrete Wavelet Transform (DWT) based image fusion algorithm applied to the images obtained from the same area. In section V, We presents the fusion of difference images. In section VI, simulation results are discussed for satellite images are shown. In section VII, the statistical analysis of the proposed algorithm is discussed and Section VIII concludes the paper.

2. IMAGE DIFFERENCE ALGORITHMS

To detect the change from multi-temporal remote sensing images, spectral changes on difference images indirectly reflect the change features and change information due to the change of pixel spectral reflectance values and provide hints to land cover changes during the observation time. In this research, Five basic algorithms to extract information based on spectral changes are implemented[14],[19],[20]. These algorithms are briefly introduced in the following paragraphs.

- Simple Differencing:

$$Y_{SD}^{i} = \left| X_{T2}^{i} - X_{T1}^{i} \right|, \qquad \text{i= 1,2,…,N} \qquad (1)$$

The Y_{SD} image is the most direct indicator of a spectral change in reflectance[20]

- Simple Ratioing:

$$Y_{SR}^{i} = \left| \frac{X_{T2}^{i}}{X_{T1}^{i}} - 1 \right|, \qquad \text{i = 1,2,…,N} \qquad (2)$$

The Y_{SR} image reflects the change information through the rationing of two images . Ratioing is immune to false positives caused by sun elevation angle, shadows and terrain, at least to some extent. After the absolute value operation, the pixels with larger values correspond to higher possibilities of change, and those pixels with a value close to 0 are hints to no-change areas.

The Y_{AD} image integrates the change information on each band into a single band through simple addition. However, this process may also cause amplification of detection errors.

Performing these algorithms, Two typical spectral difference images are extracted from a pair of multi-spectral images. Their capabilities for representing temporal changes are different from each other. The absolute distance, Euclidian distance and Chi square Transformation algorithms are also the image differencing

algorithms. By performing these algorithms with the input satellite images and doing the image fusion based on PCA and DWT will be able to get more information about the change areas.

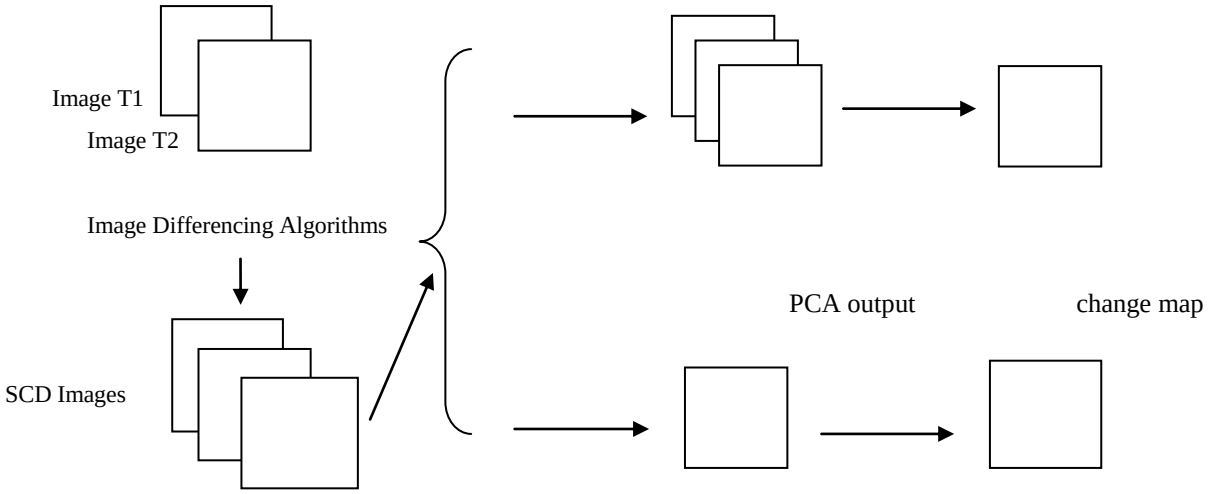

Fig. 1 . Fusion of Difference Images

3. PRINCIPAL COMPONENT ANALYSIS

In remote sensing, changes can be determined by comparing the spectral response differences at the same spatial location. For that Principal Component Analysis method [20] is performed by using a set of two or more multispectral images acquired at different times. PCA is mathematically defined as an orthogonal linear transformation that transforms the data to a new coordinate system such that the greatest variance by any projection of the data comes to lie on the first coordinate the second greatest variance on the second coordinate.

Define a data matrix, $\mathbf{X}^T$. The zero empirical mean of the distribution has been subtracted from the data set. The singular value decomposition of $\mathbf{X}$ is $\mathbf{X} = \mathbf{W\Sigma V^T}$, where the $m \times m$ matrix $\mathbf{W}$ is the matrix of eigenvectors of the covariance matrix $\mathbf{XX}^T$, the matrix $\mathbf{\Sigma}$ is an $m \times n$ rectangular diagonal matrix with nonnegative real numbers on the diagonal, and the $n \times n$ matrix $\mathbf{V}$ is the matrix of eigenvectors of $\mathbf{X}^T\mathbf{X}$.The dimentionality will be preserved by the PCA transformation i.e. gives the same no of PCs as original variables using the formula:

$$\begin{aligned} Y^T &= X^T W \\ &= V\sum{}^T W^T W \\ &= V\sum{}^T \end{aligned} \quad (3)$$

$\mathbf{V}$ is not uniquely defined in the usual case when $m < n - 1$, but $\mathbf{Y}$ will usually still be uniquely defined. Here, W is an orthogonal matrix and each row of $\mathbf{Y}^T$ is simply a linear transformation which is corresponding to the row of $\mathbf{X}^T$. The scores of the cases made up the first column of $\mathbf{Y}^T$ with respect to the PCs, the next column has the scores with respect to the 2nd PC and so on. To reduce -dimensionality representation, $\mathbf{X}$ down could be produced into the reduced space defined by only the first L singular vectors,

$$Y = W_L^T X = \sum\nolimits_L V^T \quad (4)$$

where $\mathbf{\Sigma}_L = \mathbf{I}_{L\times m}\mathbf{\Sigma}$ with $\mathbf{I}_{L\times m}$ the $L \times m$ rectangular identity matrix.

The matrix $\mathbf{W}$ (singular vectors of $\mathbf{X}$) is the matrix $\mathbf{W}$ equivalently of eigenvectors of the matrix of observed co variances $\mathbf{C} = \mathbf{X}\,\mathbf{X}^T$

$$XX^T = W\sum\sum{}^T W^T \quad (5)$$

PCA transforms Multivariate data set of inter correlated Variables into Data set of new un-correlated linear combinations of the original Generates a new set of axes which are orthogonal and Computation of

Principal Components (PCs) comprises the calculation of Covariance (un standardized PCA) or Correlation (standardized PCA) matrix, Eigen values, Eigen vectors and Principal Components(PCs). Comparing the spectral response differences at the same spatial location.

- Eigen values and Eigen Vectors Computation

To calculate the Eigen values, the following equation is used

$$|A-\lambda I| = 0 \quad (6)$$

After calculating the eigen values the calculation of eigen vectors can be found by finding non-zero solutions for the equation of the eigen values.

First, two images with the same coordinate system are obtained:

$$X = \{ Xi \mid i= 1,2, \ldots, n\} ; Y = \{ Yi \mid i= 1,2,\ldots,n\} \quad (7)$$

Different types of change information are contained in different spectral bands; thus, the use of one spectral band usually doesnot allow every type of changes to be detected.Once threshold is applied to a difference image where the change information presents at smaller magntiudes, within the range will be lost. The Principal Component w_1 of a data set X can be defined as

$$W_1 = argmaxVar\{w^T X\} = argmax\{(w^T X)^2\} \quad (8)$$

The kth component can be found by subtracting the first $K-1$ principal components from $\mathbf{X}$:

$$\hat{X}_{k-1} = X - \sum_{i=1}^{k-1} w_i w_i^T X \quad (9)$$

Substituting this as the new data set to find a PC

$$W_K = argmax\ E\{W^T X^{\wedge}_{k-i}\} \quad (10)$$

Noise could be included as change if its magnitude falls outside range. PCA can be applied to the difference images. The following is a detailed description of PCA using the covariance method . But note that it is better to use the singular value decomposition The data set **Y** of smaller dimension *L* is the Karhunen–Loève transform (KLT) of matrix **X**:

$$\mathbf{Y} = \mathbb{KLT}\{\mathbf{X}\} \quad (11)$$

The output principal component images are called principal component difference images. Computing PCA using the covariance method,

- Organize the data set

If have data comprising a set of observations of *M* variables. To reduce the data so that each observation can be described with only *L* variables, *L* < *M*. Suppose further, that the data are arranged as a set of *N* data vectors $\mathbf{X}_1 \ldots \mathbf{X}_N$ with each $\mathbf{X}_n$ representing a single grouped observation of the *M* variables.

Write $\mathbf{X}_1 \ldots \mathbf{X}_N$ as column vectors which has *M* rows of each.
Into a single matrix **X** of dimensions *M* × *N*, Common vectors should be placed.

- Emprical mean calculation.

Find the empirical mean along each dimension *m* = 1, ..., *M*.
The calculated mean values should be placed into an empirical mean vector **u** of dimensions *M* × 1

- Deviations calculation from the mean

The solution towards finding a principal component basis that minimizes the mean square error (approximating the data) is mean subtraction. Subtract the **u** from each column of the data matrix **X**. u- empirical mean.

Store **B** – mean subtracted data.

$$\mathbf{B} = \mathbf{X} - \mathbf{uh} \quad (12)$$

Where h is a 1x N row vector of all 1s:

$$h[n] = 1 \qquad \text{for } n = 1, \ldots, N \quad (13)$$

- Covarience matrix

Find the *M* × *M* empirical covariance matrix **C** from the outer product of matrix **B** with itself:

$$\mathbf{C} = \mathbb{E}[\mathbf{B} \otimes \mathbf{B}] = \mathbb{E}[\mathbf{B} \cdot \mathbf{B}^*] = \frac{1}{N-1}\mathbf{B} \cdot \mathbf{B}^* \quad (14)$$

Where
$\mathbb{E}$ is the expected value operator,
$\otimes$ is the outer product operator, and
$*$ is the conjugate transpose operator. If B consists entirely of real numbers and this is the case in many applications, the conjugate transpose is the same as the regular transpose.

- Energy for each eigenvector calculation

The Eigen values represent the distribution of the source data's energy among each of the eigenvectors, the eigenvectors form a basis for the data. The energy content calculated cumulatively, *g* for the *m* th eigenvector is the sum of the energy content across all of the Eigen values from 1 through *m*:

$$g[m] = \sum_{q=1}^{m} D[q,q] \qquad \text{for} \qquad m = 1, \ldots, M \quad (15)$$

After performing each steps the principal components of the input images are obtained in the otput image. By usiong the PCs the representation of the image features are done. In this paper, the PCA algorithm is used for the merging process of two different images for extracting the maximum possible information from the two images.

4. WAVELET TRANSFORM

In this section, We discuss about DWT based image fusion technique. The two-dimensional wavelet algorithm is an efficient algorithm, has optimal storage space and orientation sensitivity.

The 2D DWT is used in compression and it is a very modern mathematical tool for de noising and watermarking applications. It should be carefully analyzed to exploit all its advantages. This should be studied in statistical point of view. The decimation process of two images obtained at the output of the two filters has to be done with a factor of 2.
Next, The column of the images obtained are filtered with m0 at low pass filter and with m1 at high pass filter. With the decimator factor 2, the columns of those four images are also decimated. Four new sub images are generated. After 2 low pass filtering the approximation sub image called LL image is obtained. The three other detail sub images are LH,HL and HH . The input of the next iteration is represented by LL image. The coefficients of the DWT will be noted with xD_m^k. X represents the image who's wavelet is computed, m represents the iteration index and k=1, for the HH image. K=2 for the HL image and k=3 for the LH image ,k=4 for the LL image.
The computation of the coefficients are done with the following relation:

$$xD_m^k[n,p] = \langle x(T1,T2), \Psi^{\mathrm{k}}_{\mathrm{m,n,p}}(\mathrm{T1},\mathrm{T2}) \rangle \quad (16)$$

Where the wavelets can be factorized:

$$\Psi^{\mathrm{k}}_{\mathrm{m,n,p}}(\mathrm{T1},\mathrm{T2}) = \alpha^{\mathrm{k}}_{\mathrm{m,n,p}}(\mathrm{T1}).\alpha^{\mathrm{k}}_{\mathrm{m,n,p}}(\mathrm{T2}) \quad (17)$$

Using the scale function $\varphi(T)$ and the mother wavelets $\Psi\,(\mathrm{T})$ with the aid of the following relations:

$$\alpha^{\mathrm{k}}_{\mathrm{m,n,p}}(\mathrm{T}) = \begin{cases} \varphi_{\mathrm{m,n}}(\tau), \mathrm{k} = 1{,}4 \\ \psi_{\mathrm{m,n}}(\tau), \mathrm{k} = 2{,}3 \end{cases} \quad (18)$$

$$\beta^{\mathrm{k}}_{\mathrm{m,n,p}}(\mathrm{T}) = \begin{cases} \varphi_{\mathrm{m,n}}(\tau), \mathrm{k} = 2{,}4 \\ \psi_{\mathrm{m,n}}(\tau), \mathrm{k} = 1{,}3 \end{cases} \quad (19)$$

Where : $\varphi_{m,n}(\tau) = 2^{-\frac{m}{2}}\,\varphi(2^{-m}\tau - n)$ (20)

$$\psi_{m,n}(\tau) = 2^{-\frac{m}{2}}\,\psi(2^{-m}\tau - n) \quad (21)$$

A bi orthogonal wavelet is a wavelet where the associated wavelet transform is invertible but there is no need to be orthogonal. Bi orthogonal wavelets design will allow more degrees of freedom than normal orthogonal wavelets. One additional degree of freedom is the possibility to construct symmetric wavelet functions. In the bi orthogonal case, there are two scaling functions $\phi, \tilde{\phi}$, different multi resolution analyses can

be generated, and accordingly two different wavelet functions $\psi, \tilde{\psi}$. So the numbers *M* and *N* of coefficients in the scaling sequences $a, \tilde{a}$ will differ. The following bi orthogonality condition must be satisfied the scaling sequences

$$\sum_{n\in Z} a_n \tilde{a_n} + 2m = 2.\delta_{m,0} \quad (22)$$

The Daubechies D4 transform has four wavelet and scaling function coefficients. The scaling function coefficients are h0, h1, h2 and h4. To the data input, each step of the wavelet transform applies the scaling function. The original data set, which has N values, for calculating the N/2 smoothed values, the scaling function will be applied in the wavelet transform step. In the ordered wavelet transform those values are stored in the lower half of the N element input vector. The wavelet coefficient values are: $g_0 = h_3, g_1 = -h_2, g_2 = h_1, g_3 = -h_0$

Each step of the wavelet transform applies the wavelet function to the input data. If the original data set has N values, the wavelet function will be applied to calculate N/2 differences. In the ordered wavelet transform the wavelet values are stored in the upper half of the N element input vector. The scaling and wavelet functions are calculated by taking the inner product of the coefficients and four data values. The equations are shown below:

Daubechies D4 scaling function:

$$a_i = h_0 s_{2i} + h_1 s_{2i+1} + h_2 s_{2i+2} + h_3 s_{2i+3}$$

$$a[i] = h_0 s[2i] + h_1 s[2i+1] + h_2 s[2i+2] + h_3 s[2i+3];$$

Daubechies D4 wavelet function:

$$c_i = g_0 s_{2i} + g_1 s_{2i+1} + g_2 s_{2i+2} + g_3 s_{2i+3}$$

$$c[i] = g_0 s[2i] + g_1 s[2i+1] + g_2 s[2i+2] + g_3 s[2i+3]; \quad (23)\ \&\ (24)$$

The Haar wavelet is a sequence of rescaled "square-shaped" functions which together form a wavelet family or basis. Wavelet analysis is similar to Fourier analysis in that it allows a target function over an interval to be represented in terms of an ortho normal function basis. Haar used these functions to give an example of a countable ortho normal system for the space of square-integral functions on the real line. The Haar wavelet's mother wavelet function $\psi(t)$ can be described as

$$\psi(t) = \begin{cases} 1 & 0 \le t < 1/2, \\ -1 & 1/2 \le t < 1, \\ 0 & \text{otherwise.} \end{cases} \quad (25)$$

Its scaling function $\phi(t)$ can be described as

$$\phi(t) = \begin{cases} 1 & 0 \le t < 1, \\ 0 & \text{otherwise.} \end{cases} \quad (26)$$

Property of Haar wavelet is any continuous real function can be approximated by linear combinations of the shifted functions and constant function. In this paper Haar wavelet is used for the DWT process of the input satellite images.

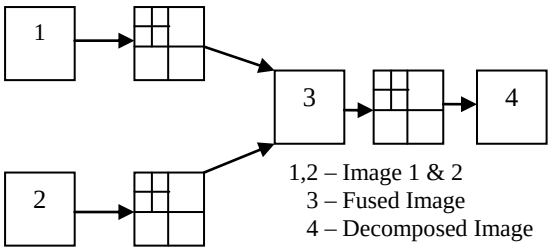

Fig.2. DWT algorithm based fusion

After performing the DWT operation with the two different input images the maximum information from the two input images are obtained by fusing the outputs.

5. FUSION OF DIFFERENCE IMAGES

The fusion process has to be done by using the output images of image differencing algorithms i.e. Simple Differencing and Simple Ratioing. Those output images are given as input to the PCA algorithm. PCA is done to the output of simple difference algorithm and simple ratioing algorithm respectively. The Simple image addition is done with the output of PCA. The PCs are found from the output image which is obtained by using the Simple differencing algorithm. The PCs are found using simple ratioing algorithm. Then the output images are fused into one image, where we can find the maximum information about the change.

Likewise, the output images of differencing and ratioing algorithm are given as input to the DWT algorithm. 2D- DWT is done to the output of simple difference algorithm and simple ratioing algorithm respectively by using the Haar wavelet, Daubechies wavelet and Bi-orthogonal wavelets. The Simple image addition is done with the outputs of DWT. The Haar wavelet is the simplest possible wavelet. The DWT based on the wavelets **Haar, Daubechies Bi - orthogonal** are performed on the images and for the analysis process the outputs of the Haar wavelet is taken.

After building multiple SCD datasets, it is able to provide hints to various change features, information fusion techniques are introduced into the change detection process to improve the reliability of the final detection result. The PCA and DWT based image fusion algorithms are therefore selected to combine the merits to improve the accuracy of detection results based on each single method.

6. STASTICAL ANALYSIS

In order to prove the effectiveness of the proposed procedure, Two datasets of Prague acquired by satellite are used as experimental data source. The assessment of the proposed method will be provided by looking at land cover change detection and affected areas after flood.

This section will consider three types of comparative analysis, such as non-superiority testing, which may be of only rare use in remote sensing and which are generalizations of the scenarios outlined will not be considered further so that the focus may be on the general nature of comparative analysis.

Statistical test of the difference in accuracy values are commonly encountered in remote sensing. For example, many studies have sought to evaluate a set of classifier and have done so on the basis of the accuracy with which they can classify data. Using this common application as a basis for discussion, this section outlines key issue sin statistical comparisons. Thus, for instance,

one of the most widely promoted means to compare classification accuracy statements in remote sensing is through the comparison of Kappa K- coefficients.

A more quantitative analysis of the results can be obtained by selecting 2824 samples of change areas and 4294 samples of no-change areas, according to the field work and data interpretation. These samples will be used to compute the accuracy values.

In order to compare the statistical significance of the difference between two individual SCD detectors or fusion strategies, a Statistical Z test have to be computed among the K coefficients. With this approach, the statistical significance of the difference between the two independent kappa coefficients will be evaluated through the calculation of a Z value. The formula used to calculate:

$$Z = \frac{K2-K1}{\sqrt{\sigma_{k2}^2-\sigma_{k1}^2}} \quad (27)$$

The calculations of Accuracy values of the test site and Statistical Significance of the Difference Between Kappa co-efficient are to be obtained for more precise statistical analysis. The most important change between two considered test areas will be connected with the Human Activities, Urbanization process and also due to disasters like Earthquake and flood. In this Paper, The Image difference algorithms and also the fusion of difference images are done with the flood affected areas of Prague. Further research will focus on fusion of multiple change indices in very high-resolution data of urban areas and implementation of some other differencing algorithms to better delineate the urban change areas. Moreover the spatial distribution of change / No-Change pixels will be considered to improve the final result.

7. SIMULATION RESULTS

The proposed algorithm is applied on satellite images from Internet and their simulation results are presented below.

(a) (b)

(c) (d)

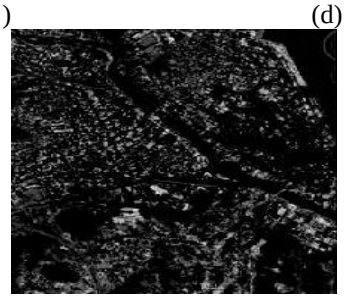

(e)

Fig 3. Simulation results of DWT – Bi orthogonal wavelet: (a) and (b) are the Input images of Japan taken before Tsunami and after Tsunami 2012;(c)Background image of DWT using bi-orthogonal wavelet; (d) Foreground image of DWT using bi-orthogonal wavelet; (e) Fused image of (c) and (d) for change detection.

(a) (b)

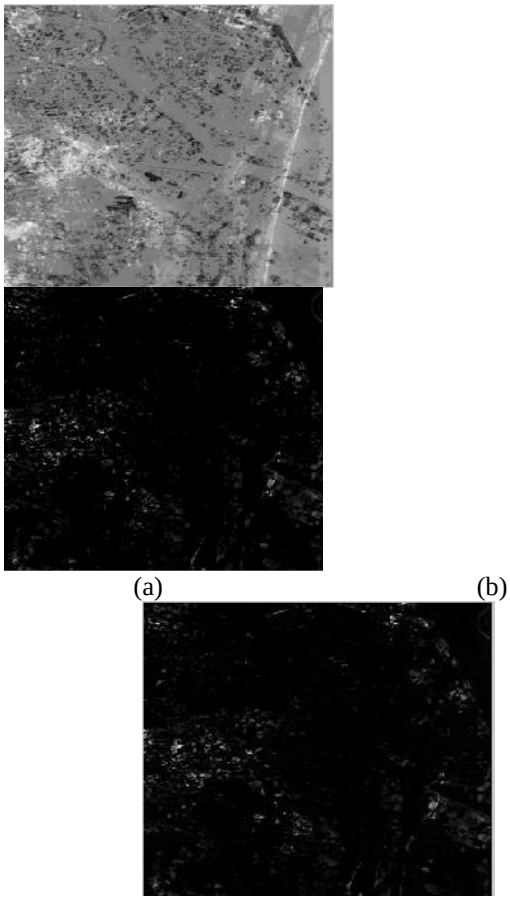

(a) (b)

(c)

Fig 4: Simulation results of DWT – Daubechies wavelet: (a) and (b) are the Input images of Japan taken before Tsunami and after Tsunami 2012;(c)Background image of DWT using Daubechies wavelet; (d) Foreground image of DWT using Daubechies wavelet; (e) Fused image of (c) and (d) for change detection

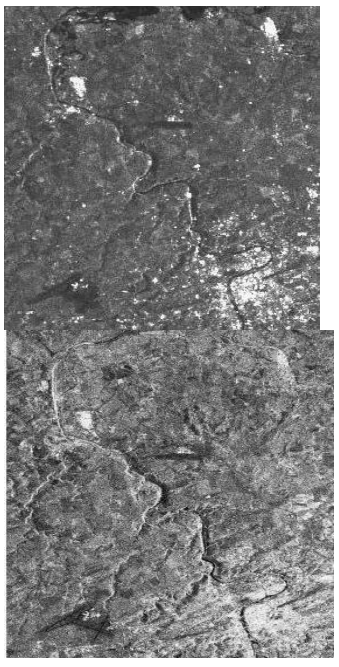

(a) (b)

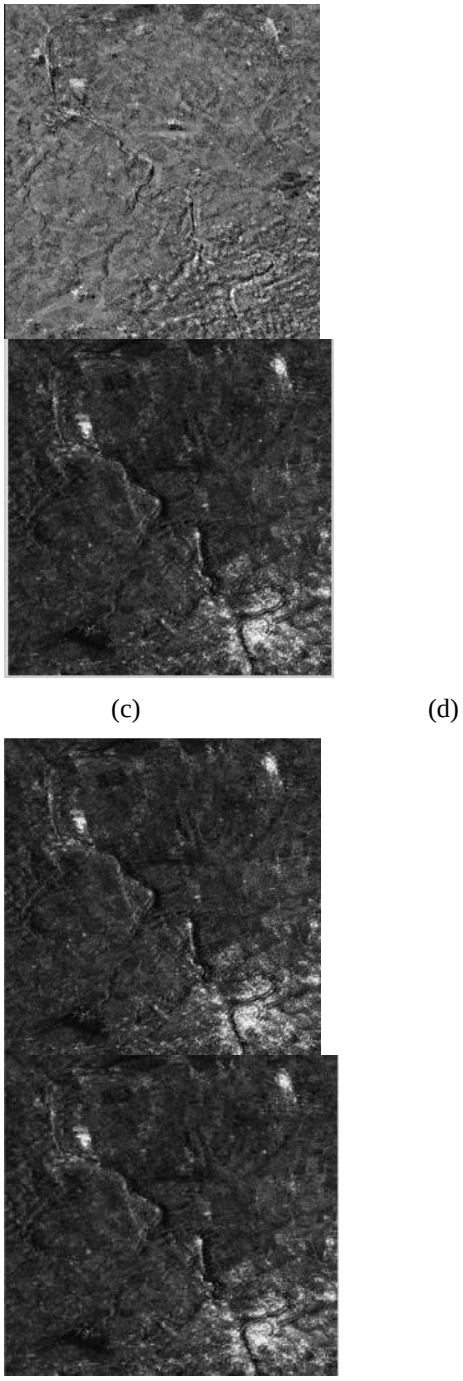

(c) (d)

(e) (f)

Fig. 5. Simulation results of Prague flood: (a) Prague before flood, (b) Prague after flood, (c) difference of the (a) and (b), (d) ratioing of the (a) and (b), (e) fused image of (c) and (d) using PCA and (f) fused image of (c) and (d) using DWT - Haar wavelet.

The three image sets of Japan i.e. before tsunami and after tsunami. The Difference algorithms, Simple Difference and Simple Ratioing are implemented by using these three different sets of images seperately and the outputs of the Differece algorithm and Ratioing algorithms are taken as inputs to the fusion algotithms.

The Image fusion Techniques based on PCA fusion and DWT based fusion are to be performed to extract the change information between the images taken of japan, before tsunami and after tsunami.

(a) (b)

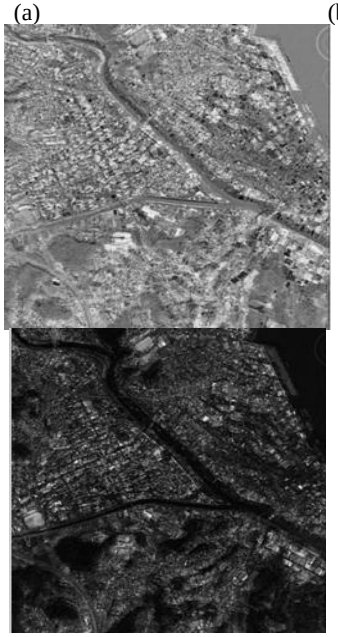

(c) (d)

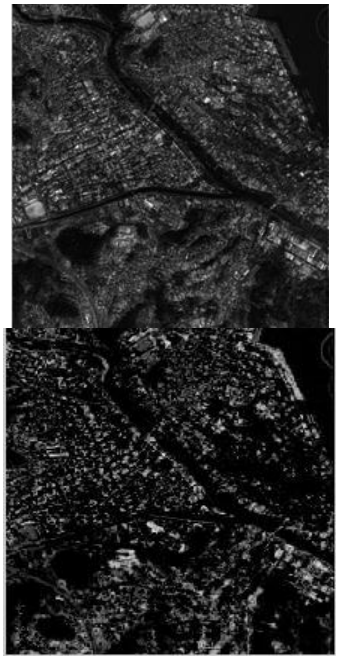

(e) (f)

Fig.6 Simulation results of Input images of Japan taken before Tsunami and after Tsunami 2012 : (a) and (b) are the Input images of Japan taken before Tsunami and after Tsunami; (c) difference of (a) and (b), (d) ratioing of (a) and (b), (e) fused image of (c) and (d) using PCA and (f) fused image of (c) and (d) using DWT - Haar wavelet

(a) (b)

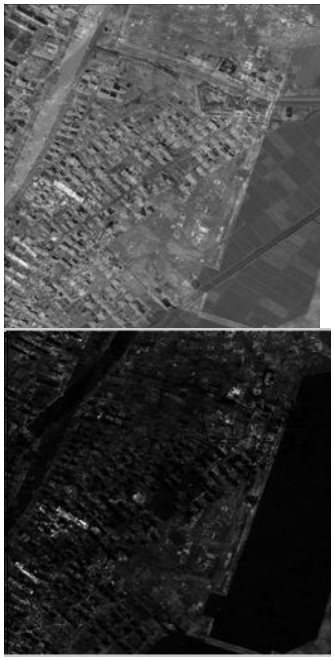

(c)

(a)

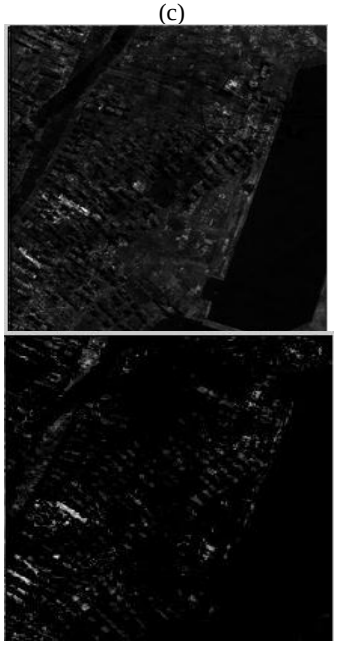

(e)

(c)

(d)

Fig.7. Simulation results of Input images of Japan taken before Tsunami and after Tsunami 2012 : (a) and (b) are the Input images of Japan taken before Tsunami and after Tsunami; (c) difference of (a) and (b), (d) ratioing of (a) and (b), (e) fused image of (c) and (d) using PCA and (f) fused image of (c) and (d) using DWT - Haar wavelet

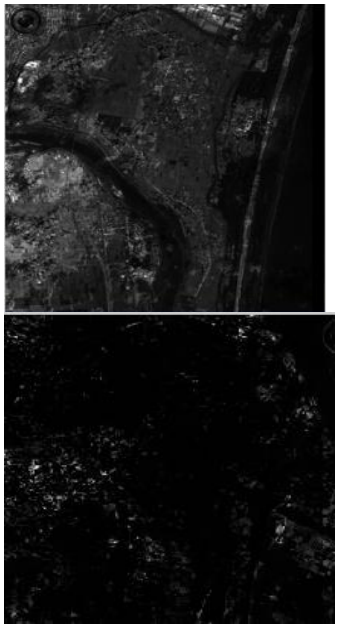

(e) (f)

Fig.8 Simulation results of Input images of Japan taken before Tsunami and after Tsunami 2012 : (a) and (b) are the Input images of Japan taken before Tsunami and after Tsunami; (c) difference of (a) and (b), (d) ratioing of (a) and (b), (e) fused image of (c) and (d) using PCA and (f) fused image of (c) and (d) using DWT - Haar wavelet

By taking the false color composites of the Different images which are taken by the Earth Observation Satellites using SAR imaging device will improve the change detection. The difference images, produced by the various difference image algorithms are not giving enough information to detect the change between the images taken before the flood in Prague and after the flood in Prague. By performing fusion of those outputs obtained from the difference algorithms, We are able to detect the change between two images taken in different times of a same area.

8. CONCLUSION

The image difference algorithms are used between the two images produces the results which are not efficient to detect the changes. Based on the large number of available techniques, remote sensing images constitute the most feasible and efficient tool for land cover change detection. Usually, change detection by comparing multiple images of the same ground area acquired at different dates.

In recent years, advances made in change detection using various pattern discovery methods have shown its importance in many real world applications. However, conventional change detection methods such as differencing and ratioing do not exploit spectral characteristics of the different land cover changes since they employ only one spectral channel. Besides, the user if often interested in complete information about the change, including positions and spatial extent, as well as the precise nature of change, which is not available with conventional change detectors.

The proposed change detection method based on fusion of multiple SCD data set is feasible and more effective for disaster monitoring than the change information extracted by single SCD algorithms. Fusion of multiple change indices in very high resolution data will lead to the betterment of change detection approach by fusion method.

9. REFERENCES

[1] Peijun Du, Senior member, IEEE, Sicong Liu, Paclo Gamba, Senior Member, IEEE, Kun Tan, and Junshi Xia, " Fusion of difference images for change detection over urban areas ", IEEE journel of selected topics in applied earth observations and remote sensing. Vol. 5, no.4, august 2012.

[2] N.Longbotham, F. Pacifici, T.Glenn, A. Zare, M. Volpi, D. Tuia,

E. Christophe, J.Michel, J. Inglada, J. Channusot, and q. Du, "Multimodal change detection, application to the detection of flooded areas: Outcome of the 2009-2010 data fusion contest," IEEE j. Sel. Topics Appl. Earth Obsrev. Remote sensing (JSTARS), vol.5, no.1. pp, 331-342, 2012

[3] D.R. Li, "Remotely sensed images and GIS data fusion for automatic Change detection." Int. J. Image and data Fusion, vol,1, no.1, pp. 99-108, 2010

[4] L. Wei, Y. Zhong, L. Zhang, an p.li, "Adaptive change method of remote sensing fusion", J. Remote Sens., vol, 14,no.6 ,pp, 1196 – 1211, 2010

[5] G. M. Foody, " Classification accuracy comparison: Hypothesis tests and the use of confidence intervals in evaluations of difference, equivalence and non- inferiority," remote Sensing. Environ, vol.113, no 8,pp, 1658 – 1663, 2009

[6] F. Bovolo, and L. Bruzzone, "A Split-Based approach to unsupervised change detection in large size multi-temporal images: Application to Tsunami-damage assessment," IEEE trans. eoScience. Remote Sens., vol. 45, no.6, pp. 1658 – 1670, 2007

[7] B. Desclee, P. Bogaert, and P. Defourny, "Forest change detection by statistical object based maethod", Remote Sens, Environ., vol. 102, no. 1-2, pp. 1- 11, 2006

[8]G. Ma, Pi Li, and Q. Qin, "Based on fusion and GGM change detection approach of remote sensing images," J.Remote ., vol 10, no.6 pp. 847 – 853, 2006

[9] S. Le Hegarat – Mascle, R. Seltz, L. Hubert – Moy, S. Corgne, and N. Stach, " Performance of change detection using remotely sensed data and evidential fusion: Comparison of three cases of application," Int. J. Remote Sens., vol. 27, no.16, pp.3315 – 3532, 2006

[10] Y. Bazi, L. Bruzzone, and F. Melgani, "An unsupervised approach based on the generalized Gaussian Model

[11] Y.Bazi, L.Bruzzone and F.Melgani,"An unsupervised approach based on the generalized Gauusian Model – to automatic change detection in multi temporal SAR images."IEEE Trans. Geosci.Remote Sens.,vol.44,no.10,pp.2828-2838,2006

[12] Guixi Liu, Wenjin Chen, Wenjie Ling,"An image fusion method based on directional contrast and area based standard deviation", Electronic Imaging and Multimedia Technology IV,edited by Chung-sheng Li, Minerva M.Yeung. Proc.of SPIE vol. 5637 0277-786X/05/$15

[13] S.Le Hegarat-Mascle and R.Seltz,: "Automatic change detection by evidential fusion of change indices,"Remote sensing.Environ.,vol.91,no.3-4,pp.390-404,2004.

[14] A.D'Addabbo,G.Satalino,G.Pasquariello, and P.Blonda, "Three different unsupervised methods for change detection: An application," in proc.2004 IEEE Int. Geoscience and remote sensing symp., IGARSS'04,sep. 20-24,2004,vol.3,pp.1980-1983.

[15] S.Le Hegarat-Mascle and R.Seltz," Automatic change detection by evidential fusion of change indices",Remote sens.Environ,vol.91, no.3-4pp.390-404,2004

[16] C.E.Woodcock,s.A.Machomber, M.Pax-lenney, and W.B.Cochen,"Monitoring largeareas for forest change detection using Land sat" Remote sensing Environ.,vol.78,no.1-2,pp.194-203,20011981,pp.278-283

[17] M.KRidd and J.J.Liu, "A comparison of four algorithms for change detection in an urban environment."Remote sens.Environvol.63,no.2,pp.95-100,1988

[18] C.Pohl and J.VanGenderen, "Multisensor image fusion in remote sensing:concepts, methods and applications."Int.J.Remote sens.,vol.19,no.5,823-854,1998.

[19] E.F. Lambin and A.H.Strahler, "Change-vector analysis in multi temporal space – a tool to detect and categorize land cover change processes using high temporal resolution data."Remote sens.Environ.,vol.48,no.2,pp.231-244,1994.

[20] P.Gong,"Change detection using Principal Component Analysis and fuzzy set theory." Can.J.Remotesense.,vol.19.no.1.pp.22-29,1993.